Proceedings of ICAPP '05
Seoul, KOREA, May 15-19, 2005
Paper 5424

Simplified Evaluation of Key Phenomena during a Complete Single-Channel Blockage Event in ACR-700

Craig D. Gerardi, Jacopo Buongiorno
Massachusetts Institute of Technology
77 Massachusetts Avenue, Cambridge, 02139-4307 MA
Tel: (617)253-7316*, Email: jacopo@mit.edu*

Abstract – *The severe flow blockage accident in the ACR-700 has been analyzed using simplified one-dimensional models. The scenario is studied from initial complete flow blockage in a single pressure tube (PT) through coolant boiloff, fuel heat up, and cladding melt to molten cladding/PT interaction and subsequent PT rupture. It was found that coolant boiloff occurs within 3 s, cladding melt within 10 s, and PT rupture within 12 s of accident initiation, which is consistent with more complex models found in the literature. Our results represent a solid physical basis for the more sophisticated models that will be needed for licensing analyses of the severe flow blockage event in ACR-700.*

I. INTRODUCTION

The ACR-700 is an advanced pressure-tube (PT) reactor being developed by Atomic Energy of Canada Limited (AECL). As in conventional CANDU reactors, the PTs are horizontal and each accommodates 12 short circular fuel assemblies (FAs). Each PT is surrounded by a calandria tube (CT). The space between the CTs is filled with the heavy-water moderator. Unlike traditional CANDUs, however, the ACR-700 utilizes slightly enriched uranium fuel and light-water coolant in lieu of natural uranium fuel and heavy-water coolant. Also, the operating temperatures and pressure have been increased to enhance the thermal efficiency. AECL has recently completed pre-application of ACR-700 with the U.S. Nuclear Regulatory Commission.

One postulated accident scenario for ACR-700 is the complete coolant flow blockage of a single PT. The flow is not monitored within each individual PT, thus during the early stages of this accident the reactor remains at full power, resulting in rapid coolant boil-off and fuel overheating. Melting of the Zircaloy components of the fuel bundle (cladding, end plates and end caps) can occur, with relocation of some molten material to the bottom of the PT. The hot spot caused by the molten Zircaloy/PT interaction may cause PT failure due to localized plastic strains. PT failure results in depressurization of the primary system, which triggers a reactor scram, after which decay heat is removed via reflooding, thus PT breach effectively terminates the accident. Clearly, prediction of the PT time-to-failure is of great importance for this accident.

The purpose of this paper is to present a very simple analysis to predict the PT time-to-failure following a complete flow blockage. The analysis describes the key phenomena involved in the sequence, and represents a solid physical basis for developing more complex models that can be used for licensing purposes.

II. OVERVIEW OF PHENOMENA CONSIDERED

A brief overview of the sequence steps considered and their associated key phenomena is provided in Table I**Error! Reference source not found.**.

Table I: Key steps considered and associated phenomena.

Sequence	*Phenomena*
Coolant Boiloff	• Energy of Evaporation
Fuel Pin Heatup / Cladding Melt	• Energy Redistribution • Fission Heat • Radiative Heat Transfer • Convective Heat Transfer • Zr/Steam Chemical Reaction • Wetting Effects Preventing Molten Zr Relocation
Molten Zr/PT Interaction	• Zr Solidification • Radiative Heat Transfer • Convective Heat Transfer • Zr/Steam Chemical

	Reaction • Conduction Between Zr/PT
PT Failure	• Creep Strain

A summary description of the models and results follows. A complete description of the models will be published in report form later this year.

III. COOLANT BOIL-OFF

The postulated initiator for this scenario is a complete (e.g. 100%) blockage of flow at the inlet of a single PT. The reactor remains at full power and pressure (12.6 MPa) since flow is not monitored in individual PTs. The flow of water into the PT is assumed to cease upon accident initiation causing coolant vaporization to occur almost immediately.

Using a heat of evaporation of 1321 kJ/kg and a peak channel power of 7.293 MW, it was calculated that the coolant inventory completely evaporates in about 2.8s.

IV. ENERGY REDISTRIBUTION WITHIN THE FUEL PIN

Once a fuel pin is uncovered, the convection coefficient becomes very low, and radiative heat transfer to the surrounding pins and the PT wall is also negligible in the first few seconds of the ensuing heat-up. Thus, the radial temperature profile within the fuel flattens rapidly. This energy redistribution occurs with a time constant of 1.4 s, which was calculated by solving the transient heat conduction equation for the fuel pin with the assumptions of negligible cladding thermal capacity and thermal resistance (thin cladding), and negligible gap resistance ('collapsed' cladding). This means that roughly 1.4 s after a pin is uncovered, its cladding reaches a temperature equal to the radial average of the UO_2 temperature prior to the accident initiation. This temperature is about 680°C, and was calculated with the Babcock and Wilcox UO_2 thermal conductivity correlation [1] for a fuel pin operating at 37.9 kW/m linear power, which is estimated to be the peak linear power for ACR-700. Therefore, 680°C is the initial condition for the fuel pin heat-up calculations that follow.

V. CLADDING MELT

The fuel pin of maximum linear power is considered to begin heating up upon uncovery. The governing equation includes three terms: fission energy production, radiation heat loss and an energy storage term:

$$\rho C_p \frac{\pi}{4} D^2 \frac{dT}{dt} = q'_f - \pi D \varepsilon \sigma (T^4 - T_\infty^4) \qquad (1)$$

where ρ,C_p, D, q'_f, ε, σ, and T_∞ are the density, heat capacity, diameter of the pin, maximum linear heat generation rate, emissivity of the cladding, Stefan-Boltzmann constant, and the surroundings temperature respectively.

The values of the parameters used in the calculations are listed in Table II**Error! Reference source not found.**. The upper PT wall temperature is assumed to be a suitable representative surroundings temperature for the purpose of calculating radiation heat transfer. During the severe flow blockage event this temperature is of the order of 500°C, as found in the ACR-700 Severe Flow Blockage PIRT [2]. A sensitivity analysis has shown that our results are not very sensitive to this temperature, so a very accurate value is not necessary.

Table II: Parameters used in the calculations

Parameter	Value
Thermal Power (MWth)	1980
Gross Electric Power (nominal) (MWe)	731
Reactor Pressure (MPa)	12.6
Nominal Coolant Inlet Temperature (ºC)	279
Nominal Coolant Outlet Temperature (ºC)	325
Length of Fuel Bundle (mm)	459.3
Number of Bundles per Fuel Channel	12
Number of Fuel Channels (PTs)	284
Pressure Tube Inner Radius (mm)	51.689
Pressure Tube Outer Radius (mm)	58.169
Number of Fuel Elements per Channel	43
Lattice Pitch (mm)	220
Fuel Pin Outer Diameter (mm)	11.5
Peak Power of a Single Pin (kW)	219
Maximum Linear Heat Generation Rate (kW/m)	37.9
Peak Channel Power (MW)	7.293
Melting Temperature of Zr (ºC)	1760
Melting Temperature of UO_2 (ºC)	2850
Initial Average Fuel Pin Temperature (ºC)	680
Upper PT Wall Temperature (ºC)	500
Fuel Density (95% Theoretical) (kg/m^3)	9186

Average Fuel Thermal Conductivity (W/mK)	3.64
Fuel Heat Capacity (J/kgK)	247
Emissivity of Cladding	0.80

Solving Equation (1), it was found that the Zircaloy cladding reaches its melting temperature in approximately 10 seconds when radiation cooling is considered and approximately 6.7 seconds not including radiation heat loss (Figure 1). It is expected that the actual melting time of the cladding will lie between these two values since the topmost pins will be uncovered first but also will be cooled through radiation losses better, compared to inner pins. UO_2 melt would occur later, due to its higher melting point.

VI. WETTING EFFECTS PREVENTING MOLTEN CLADDING RELOCATION TO THE BOTTOM OF THE PRESSURE TUBE

The amount of oxygen present at the interface of the Zircaloy cladding and UO_2 at the time of Zircaloy melting greatly influences the progression of the accident; i.e., molten Zircaloy wets UO_2 in the presence of oxygen [3]. This can prevent molten Zr relocation from the cladding to the bottom of the PT. If this happens, the Zircaloy end caps and end plates will eventually melt and relocate on the PT, but this would prolong the accident and likely generate more molten material. Oxygen can diffuse to the cladding/fuel interface from the oxide layer on the outer surface of the cladding (due to the Zirconium/Steam reaction) or from the UO_2 pellet.

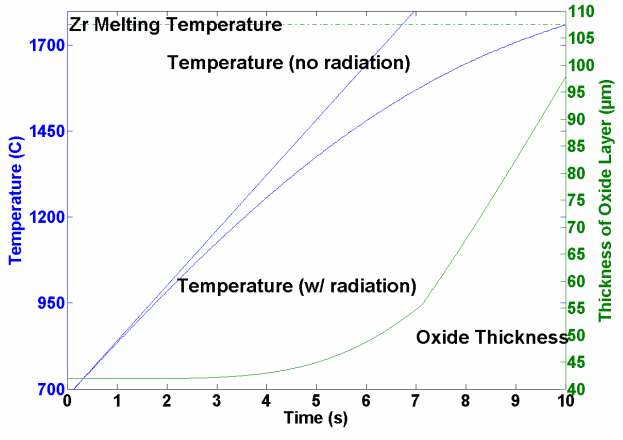

Figure 1: Oxide Layer Thickness and Cladding Temperature Profile during Fuel Heat-up

The Zirconium/Steam reaction is exothermic and releases hydrogen[1]:

$$Zr + 2H_2O \rightarrow ZrO_2 + 2H_2 + 587\ {}^{kJ}/_{mol\ Zr} \qquad (2)$$

The oxidation rate for Zircaloy-4 in steam is given by Urbanic [4]:

$$\frac{d\xi}{dt} = \frac{\delta^2}{2\xi} \qquad (3)$$

where ξ is the thickness of the region through which oxygen has penetrated and $\delta_{\xi T}$ is a temperature-dependent factor:

$$\delta_{\xi T} = 0.363e^{\left(\frac{-8968}{T}\right)} \qquad (4)$$

in the temperature range 1050-1580 °C, and

$$\delta_{\xi T} = 0.251e^{\left(\frac{-7764}{T}\right)} \qquad (5)$$

in the temperature range 1580-1850 °C.

Using the temperature curve in Figure 1, and Equations (3), (4) and (5), the growth of the oxide layer can be calculated and is also shown in Figure 1. The overall thickness of the oxide layer expected by the time of melt is approximately 97µm, or 16 percent of the overall thickness of the cladding. In this calculation, we made the assumption that at the time of the accident the cladding thickness is already 10% oxidized. Likely this is a significant overestimate of the actual initial oxidation, because CANDU FAs are not kept in reactor long enough to develop such high oxidation. However, a sensitivity analysis has shown that the final value of the oxide layer thickness is fairly independent from the initial value, because of the form of Equation (3). Thus, we have demonstrated that oxygen penetration into the cladding due to Zirconium/steam oxidation has negligible impact on molten Zircaloy-4 relocation to the PT bottom.

The second phenomenon resulting in increased oxygen content within the fuel cladding is the dissolution of solid UO_2 by molten Zircaloy-4 cladding. The driving force for this reaction is the diffusion of oxygen from the UO_2 into the cladding. This reaction predominantly occurs above

[1] Incidentally, we shall notice that the contribution of this reaction to the fuel pin heatup is completely negligible with respect to the fission heat.

the melting point of Zircaloy-4 (1760 ºC). Rosinger et al. [5] observed that molten Zircaloy does not wet UO_2 if the heating rate is sufficiently high, i.e., there is very little time for UO_2 to dissolve in the Zircaloy. The critical heating rate in their experiments was around 35 °C/s [5]. Further, Dienst et al [6] showed that the interaction of molten Zircaloy-4 with UO_2 at 1800°C in an inert atmosphere is insignificant for the first 80 s. Because the heating rate during the complete flow blockage is very high (about 140 °C/s, as seen in Figure 1) and the duration of the cladding heat-up is very short (<10 s, as seen in Figure 1), it can be concluded that, upon reaching its melting temperature, the majority of unoxidized Zircaloy-4 melts and drips from the fuel rod onto the surface of the PT. This is a remarkable finding that warrants accurate experimental verification, given its importance in the analysis of the complete flow blockage event for ACR-700.

In contrast, for longer transients with comparatively low heating rates such as a large-break loss of coolant accident (LB-LOCA) with failed emergency core cooling system (ECCS), there is sufficient time for the molten cladding to wet UO_2, and not drip as discussed in Rosinger et al [5]

VII. INTERACTION BETWEEN MOLTEN CLADDING AND PT

Once the molten cladding has relocated to the bottom of the PT, the situation can be represented as small droplets of liquid Zircaloy in contact with the Zr-2.5wt% Nb PT. The PT surface has an outer layer of zirconium oxide due to the length of service and the favorable thermodynamics of zirconium oxidation over niobium oxidation. The contact angle, θ, between ZrO_2 and molten Zircaloy-4 is approximately 120 degrees (see Figure 2), which was estimated from the contact angle data for molten zirconium droplets on various oxides in reference [7]. Using this value and the properties of molten Zircaloy, we developed and benchmarked a model, based on the Young-Laplace equation [8], to determine the geometry (height, surface area, and contact diameter) for various droplet masses.

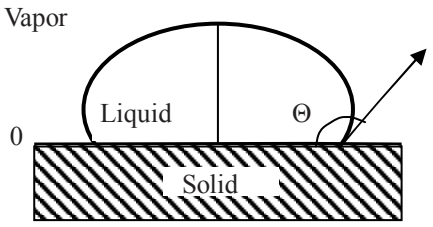

Figure 2: Contact angle for equilibrium solid-liquid-vapor system

Surface and volume information for the droplet can then be used in the energy balance for the interaction between the droplet and the PT wall:

$$\dot{E}_{storage} = \dot{E}_{chemical} - \dot{E}_{conduction} - \dot{E}_{convection} - \dot{E}_{radiation} \quad (6)$$

Equation (6) states that energy is transferred from the droplet to the PT (conduction), coolant (convection and radiation), while more energy is produced by Zr/steam reaction. To evaluate the relative importance of these energy transfer mechanisms, an order-of-magnitude comparison was performed for droplets of various mass (Table III**Error! Reference source not found.**). From this comparison, it is clear that convective and radiation energy losses are irrelevant for this problem. Zr/Steam reaction energy production is less than the energy required to complete solidification, but may need to be considered in a detailed analysis. Most energy is transferred from the droplet to the PT by conduction, as expected.

Table III: Relative Importance of Energy Transfer Mechanisms for Molten Zr/PT Interaction.

Droplet mass (g)	Convective Energy[2] (kJ)	Radiation Energy[3] (kJ)	Chemical Energy (kJ)	Solidification Energy (kJ)	Conduction Energy (kJ)
0.1	0.0003	0.0002	0.0077	0.0224	0.0296
1	0.0050	0.0042	0.0662	0.2240	0.2810
10	0.0579	0.0487	0.4847	2.2400	2.6181
100	0.4368	0.3671	3.1464	22.400	24.742

The values in**Error! Reference source not found.** Table III were obtained for the solidification times reported in Table IV, which were calculated as explained next. The interface temperature, or contact temperature between the molten Zircaloy and the PT wall was estimated as:

[2] Assumes film boiling on the surface of the droplet.
[3] Radiation through the vapor film.

$$T_w = \frac{(k\rho C_p)_{clad}^{1/2} T_{clad,i} + (k\rho C_p)_{PT}^{1/2} T_{PT,i}}{(k\rho C_p)_{clad}^{1/2} + (k\rho C_p)_{PT}^{1/2}} \qquad (7)$$

where T_w, k, $T_{clad,i}$, $T_{PT,i}$ represent the interface temperature, thermal conductivity, initial cladding temperature, and the initial PT wall temperature respectively. Equation (7) is the standard form of the interfacial contact temperature between two semi-infinite solids at different initial temperatures [9].

This approximation assumes that prior to contact, the PT wall is at 328 ºC[4] [2], while the molten metal is at 1760 ºC. The interface temperature is then found to be 995 ºC from Equation 7.

To determine the time needed for full solidification of the droplet, a simple one dimensional model characterizing the energy balance at the freezing front was developed as shown in shown in Figure 3.

The heat flux through the solid front is given by:

$$q'' = \frac{k_s}{\delta_s}(T_{melt} - T_w) \qquad (8)$$

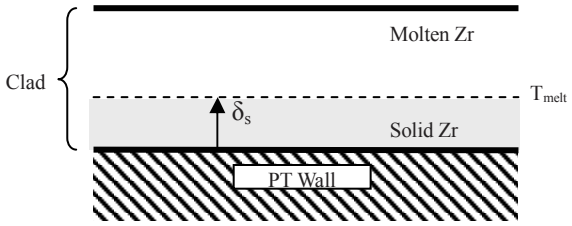

Figure 3: One Dimensional Freezing Front Model

where q", k_s, δ_s, T_{melt}, and T_w are the heat flux at the freezing front, thermal conductivity of the solid Zircaloy, thickness of the solid front, melting temperature of Zircaloy, and the PT wall temperature respectively.

Thus, the energy balance at the solidification front is:

$$\rho_s h_{ls} d\delta_s = \frac{k_s}{\delta_s}(T_{melt} - T_w)dt \qquad (9)$$

[4] Due to flow stratification, some residual liquid coolant is still present in the channel, so the bottom of the PT stays at relatively low temperature, even after the top of the PT has heated up considerably.

The heat of fusion of Zircaloy, h_{ls}, is 224 kJ/kg [10], its thermal conductivity, k_s, is 50 W/mK, and its density, ρ_s, is 6500 Kg/m^3. Equation (9) can be integrated to solve for the time required to solidify the entire thickness of the droplet:

$$t_{solidify} = \frac{\delta_s^2 \rho_s h_{ls}}{2k_s(T_{melt} - T_w)} \qquad (10)$$

Several representative times for complete solidification are given in Table IV**Error! Reference source not found.**. Note that even relatively large droplets release most of their energy within less than 2 s.

Table IV: Time to Complete Solidification for Representative Droplets

Droplet weight (g)	Thickness of droplet (mm)	Time to solidify (s)
0.1	2.3	0.157
1	4.3	0.547
10	6.8	1.369
100	7.9	1.847

The heat-up of the PT wall underneath the droplet was modeled as simple one-dimensional heat conduction as shown in Figure 4, where the inner surface of the PT wall is being heated via contact with the molten Zircaloy, while heat transfer at the outer surface of the PT is assumed negligible. The latter assumption is accurate if the PT has not yet ballooned into contact with the calandria tube. The PT/CT contact situation has not been studied yet in this project.

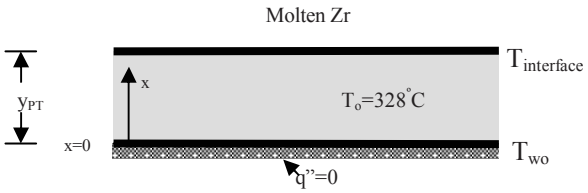

Figure 4: Diagram of 1-D Transient Conduction in PT Wall

The transient conduction problem can be solved and the temperature profile over time for various locations along the thickness of the PT may be obtained. The temperature history for the middle of the PT is shown in Figure 5.

VIII. LOCALIZED CREEP STRAIN IN PT WALL

In the region of contact with the molten Zircaloy, the PT wall will quickly reach high temperatures, develop high localized plastic strains, and eventually fail. Shewfelt [11] describes a high-temperature creep model for Zr-2.5 wt% Nb.

In the temperature range from 450ºC to 850ºC the creep rate is

$$\dot{\varepsilon} = 1.3x10^{-5}\sigma^{9}e^{(-36600/T)} + \frac{5.7x10^{7}\sigma^{1.6}e^{(-29200/T)}}{\left[1+2x10^{10}\int_{t_1}^{t} e^{(-29200/T)}dt\right]^{.42}} \quad (11)$$

and in the temperature range of 850-1200 ºC it is:

$$\dot{\varepsilon} = 10.4\sigma^{3.3}e^{(-19600/T)} + \frac{3.5x10^{4}\sigma^{1.4}e^{(-19600/T)}}{\left[1+274\int_{t_2}^{t} e^{(-19600/T)}\cdot(T-1105)^{3.72}dt\right]} \quad (12)$$

where $\dot{\varepsilon}$, σ, t_1, and t_2 are the creep strain rate, applied stress (MPa), time where the temperature is above 450°C, and time where the temperature is above 850°C respectively.

The temperature curve of Figure 5 was input into Eqs. (11) and (12), and used to find the strain at any given time using an explicit integration scheme:

$$\varepsilon_{i+1} = \varepsilon_i + \dot{\varepsilon}_i \cdot \Delta t \quad (13)$$

The circumferential (hoop) stress was calculated as:

$$\sigma_H = \frac{\mathrm{P}\cdot \mathrm{r}}{y} \quad (14)$$

where P, r and y are the pressure, inner radius of the PT, and thickness of the PT respectively.

The hoop stress is equal to 102 MPa for the nominal ACR-700 pressure of 12.6 MPa. The predicted creep strain in the middle of the PT wall is also shown in Figure 5.

The criterion for PT wall failure is 100% "true strain", suggested by AECL [12] which is defined as:

$$\varepsilon_t = \ln\frac{y+\delta}{y} \quad (15)$$

where δ represents the change in thickness of the PT.

A true strain of 100% corresponds to an engineering strain (ε=δ/y) of 1.72, using an infinite plane approximation where the volume is proportional to the thickness times the length of the plate. From Figure 5, the PT wall is expected to fail approximately 2.0 seconds from time of molten Zircaloy contact.

IX. CONCLUSIONS & FUTURE WORK

The single-channel complete flow blockage event in ACR-700 results in rapid overheating of the fuel pin, melt of the cladding and can fail the pressure tube within several seconds of accident initiation. Perhaps counterintuitive – quick failure of the PT is desirable because upon failure, the calandria tube will pressurize resulting in accident detection and scram. Thus, the quicker the PT is breached, the shorter the accident and the amount of molten material produced, which also limits failure propagation from the initially-affected PT to the surrounding PTs.

A summary of the important representative time scales calculated with our simple models for this accident is given in Table V**Error! Reference source not found.**. The total accident time range of 9-12 seconds and each of its components are consistent with the figures given in the ACR-700 PIRT [2]. Also, the range of 7-10 seconds until the beginning of some channel deformation is within the range given by the PIRT of 8 seconds. Overall, these simplified one-dimensional results have exceptionally good agreement with the findings of the much more sophisticated calculations used by AECL. These results should give confidence in verification of AECL's tools for analyzing this accident scenario and give better understanding to the individual segments of this accident.

Table V: Important Time Scales in Single-Channel Flow Blockage Event

Process	Time (s)
Coolant inventory boil-off	2.8
Fuel cladding melt	6.7-10
Molten Zr contact with PT until PT failure	2.0
Total: accident initiation to PT failure	9-12

Development of a three-dimensional detailed finite-element model for the molten Zircaloy/PT interaction is underway. This model will include the mechanisms identified as important by the simplified models, namely conduction, solidification, Zr/steam chemical reaction and localized plastic strains and failure. From further refinement of the simple models and development of the finite-element model we expect to identify possible research gaps and thus recommend additional separate effect or integrated experiments to advance the understanding of the key phenomena involved in this accident.

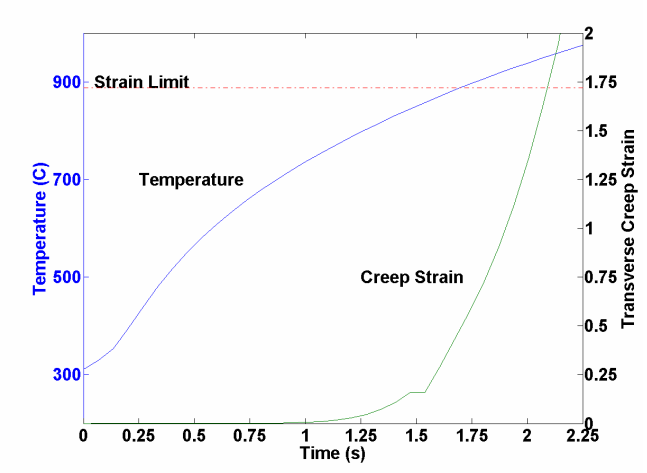

Figure 5: Predicted Transverse Creep Strain and Temperature in Middle of PT Wall with Internal Pressure of 12 MPa

ACKNOWLEDGMENTS

This work was supported by the U.S. Nuclear Regulatory Commission (NRC) through Collaborative Agreement NRC-04-02-079.

NOMENCLATURE

C	heat capacity
D	diameter
P	pressure
T	temperature
h	heat of fusion
k	heat transfer coefficient
m	mass
q'	linear heat generation rate
q"	heat flux
$\dot{q}$	power generation/energy production rate
r	radius
t	time
y	thickness of PT

Subscript

0	initial
clad	cladding
f	fission
i	initial
i	step
melt	melting of Zr
o	initial
PT	pressure tube
s	solid
t	true engineering strain
w	wall
∞	environment

Greek

δ	oxide growth constant
δ	solidification thickness
δ	change in length
ε	emissivity
ε	strain
$\dot{\varepsilon}$	strain rate
ρ	density
σ	applied stress (MPa)
σ	Stefan-Boltzmann constant (5.67e-8 W/m^2K^4)
θ	angle
ξ	oxide thickness

REFERENCES

1. N.E. Todreas and M. S. Kazimi, *Nuclear Systems I: Thermal Hydraulic Fundamentals*. Taylor & Francis. 1993.
2. PIRT for Single-Channel Severe Flow Blockage in ACR-700, AECL, Licensing Submission to U.S. NRC, February 2004, 108US-03500-LS-002, Revision 0.
3. P. Nikolopoulos, G. Ondracek, D. Sotiropoulou., "Wettability and Interfacial Energies Between Zirconia Ceramic and Liquid Metals," Ceramics International. **15**, 201-206 (1989).
4. V.F. Urbanic, T.R. Heidrick, "High Temperature Oxidation of Zircaloy-2 and Zircaloy-4 in Steam," *J. Nuclear Materials,* **75**, 251-261 (1978).
5. H. E. Rosinger, R.K. Rondeau, K. Demoline and K.J. Ross, "The Interaction and Dissolution of Solid UO2

by Molten Zircaloy-4 Cladding in an Inert Atmosphere or Steam," Proceedings of the 6th Annual Conference of the Canadian Nuclear Society. AECL Ltd., 16.33-16.38 (1985).

6. W. Dienst, P. Hofmann, D.K. Kerwin-Peck, "Chemical Interactions between UO_2 and Zircaloy-4 from 1000 to 2000 ºC," *J. Nuclear Technology*, **65,** 109-124 (April 1984).
7. S. Beer, *Liquid Metals: Chemistry and Physics*. 161-212, Marcel Dekker, Inc., New York, New York. (1972). .
8. A. W. Adamson. *Physical Chemistry of Surfaces*. 6-30, Wiley, New York, New York. (1997).
9. F.P. Incropera, D.P. Dewitt, Fundamentals of Heat and Mass Transfer, 268-272, John Wiley & Sons (2002).
10. J.R. Ramsay, "Thermal Simulation of Molten-Material/Pressure-Tube Interaction in a CANDU Nuclear Reactor," AECL, Pinawa, Manitoba, Canada.
11. R.S.W. Shewfelt, L.W. Lyall and D.P. Godin, "A High-Temperature Creep Model for Zr-2.5 wt% Nb Pressure Tubes," *J. Nucl. Materials,* **125**, 228-235 (1984).
12. R.W.L. Fong, C.K. Chow, "High Temperature Transient Creep Properties of CANDU Pressure Tubes", Presented at the 23rd Annual Conference of the Canadian Nuclear Society, Toronto, ON, AECL-12143, (June 2002).